

Review

Characterization of MoVTeNbO_x Catalysts during Oxidation Reactions Using *In Situ/Operando* Techniques: A Review

Soe Lwin, Weijian Diao, Chinmoy Baroi, Anne M. Gaffney and Rebecca R. Fushimi *

Biological and Chemical Processing Department, Energy and Environmental Science and Technology, Idaho National Laboratory, Idaho Falls, Bonneville, ID 83415, USA; soe.lwin@inl.gov (S.L.); weijian.diao@inl.gov (W.D.); chinmoy.baroi@inl.gov (C.B.); anne.gaffney@inl.gov (A.M.G.)

* Correspondence: rebecca.fushimi@inl.gov; Tel.: +1-208-526-0754

Academic Editor: Juan J. Bravo-Suarez

Received: 5 January 2017; Accepted: 6 April 2017; Published: 8 April 2017

Abstract: Light alkanes are abundant in shale gas resources. The bulk mixed metal oxide MoVTe(Sb)NbO_x catalysts play a very important role in dehydrogenation and selective oxidation reactions of these short hydrocarbons to produce high-value chemicals. This catalyst system mainly consists of M1 and less-active M2 crystalline phases. Due to their ability to directly monitor the catalysts under the relevant industrial conditions, *in situ/operando* techniques can provide information about the nature of active sites, surface intermediates, and kinetics/mechanisms, and may help with the synthesis of new and better catalysts. Sophisticated catalyst design and understanding is necessary to achieve the desired performance (activity, selectivity, lifetime, etc.) at reasonable reaction conditions (temperature, pressure, etc.). This article critically reviews the progress made in research of these MoVTe(Sb)NbO_x catalysts in oxidation reactions mainly through *in situ/operando* techniques and suggests the future direction needed to realize the industrialization of these catalysts.

Keywords: MoVTe(Sb)NbO_x; *operando*; oxidative; dehydrogenation; ethylene; acrylonitrile; ammoxidation; acrylic acid; *in situ*; characterization

1. Introduction

The domestic fossil feedstock in recent years is shifting towards light hydrocarbons due to the abundance of shale gas from hydraulic fracturing [1]. This shift induces a need for greater flexibility in both new and existing processing plants to produce consumer products (polymers, paints, lubricants, etc.) from new feedstocks. The oxidative catalytic reactions operate at milder conditions than the processing of feedstocks through steam cracking [2,3]. The conversion of light feedstocks (C₃ and shorter hydrocarbons) to high-value chemicals through highly-selective catalysts in the presence of oxygen plays a crucial role in eliminating wastes, reducing greenhouse gas emissions, and lowering market prices. Among all catalysts for light hydrocarbon processing through oxidation reactions, bulk mixed metal oxides, such as MoVTe(Sb)NbO_x catalysts, are the most promising due to their performance under favorable reaction conditions (temperature, pressure, etc.) [2,4].

The MoVTe(Sb)NbO_x catalyst system was, in the early days, reported by scientists at Mitsubishi Chemicals in the early 1990s for (amm) oxidation of propane to acrylonitrile and acrylic acid [5,6]. This catalyst generally consists of M1 and M2 crystalline phases and minor amounts of other phases, such as MoV, MoTe, Mo₅O₁₄, etc. [7–10]. The orthorhombic M1 phase is composed of pentagonal rings connected by corner sharing MO₆ octahedrons (M = Mo, V) in the (001) plane to form hexagonal and heptagonal rings with Te–O units. Its schematic representation is shown in Figure 1. The M2 phase has pseudo-hexagonal rings hosting Te–O units without any pentagonal or heptagonal rings

in the (001) plane [10,11]. The M1 phase was claimed to be obtained over the compositional range of $\text{MoV}_{0.14-0.22}\text{Te}_{0.1-0.2}\text{Nb}_{0.1-0.2}\text{O}_x$ [12]. It is speculated that the introduction of Nb causes the evolution of M2 to M1 since it serves as a template for the formation of pentagonal and heptagonal rings [13,14]. In another study, formation of the M1 phase was not observed without V, Nb, or Te in the synthesis mixture, although a high concentration of Te led to the replacement of M1 by the less active/inactive M2 phase [12]. The M1 phase is generally agreed to be active for oxidative dehydrogenation of light alkanes, although the presence of M2 is reported to aid in the activity of other oxidation reactions, such as ammoxidation of propane/propylene and oxidation of propane to acrylic acid [15,16]. Although the elemental composition of the catalysts is fixed before the reaction, the surface/bulk compositions, structures, and oxidation states change based on the type of reactants exposed, reaction time, and conditions [17].

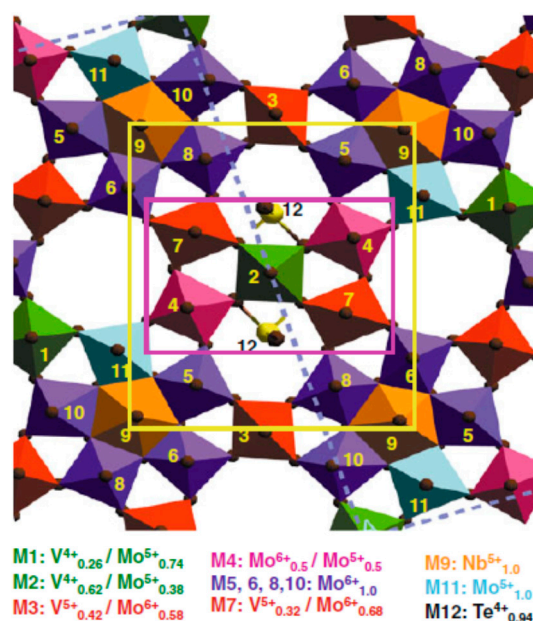


Figure 1. Schematic representation of the structure of M1 along the (001) direction. Green represents NbO_7 , blue MoO_6 and yellow MO_6 ; M = Mo or V. Figure reproduced with permission from [18].

State-of-the-art *in situ/operando* techniques along with transient kinetics can revolutionize the development of catalysts by providing information about the nature of active sites, intermediates, and kinetics under realistic industrial conditions. Only through detailed understanding of these catalyst behaviors can new synthesis methods be developed that will improve reactivity, selectivity, and lifetimes of these catalysts. In this review, dynamic changes of this mixed oxide catalyst during the reaction (such as changes in surface composition, oxidation states, acidity, etc.) are discussed mainly from knowledge and insights obtained from these *in situ/operando* approaches. The most common oxidation reactions driven by the MoVTNbO_x catalysts and studied under *operando/in situ* conditions to be discussed here are: (1) oxidative dehydrogenation of light alkanes (ethane and propane); (2) propane ammoxidation to acrylonitrile; and (3) selective oxidation of propane to acrylic acid.

2. Operando Techniques

Catalyst structures change depending on reaction temperature, pressure, and time on stream. In order to establish the structure-reactivity/selectivity relationships, which can guide the synthesis of better catalysts, characterization must be done *in situ* under relevant high-temperature/pressure industrial conditions. *In situ* cells/reactors are designed so that they can withstand such conditions, while allowing for spectroscopy/microscopy data to be taken through a window. Simultaneous measurements of the reactants and products through MS/GC must also be made to understand the

whole reaction phenomena. The term *operando* (Latin word for ‘working’) was coined by Miguel Bañares in 2002 and *operando* spectroscopy/microscopy combines an *in situ* cell with simultaneous online product analysis [19]. In these *in situ* and *operando* applications, the analytical techniques used to analyze surface and bulk catalyst structures, adsorbates, and intermediates include both spectroscopy (Raman, IR, UV-VIS, XAS, XRD, LEIS, XPS, EPR, NMR, neutron diffraction, etc.) and microscopy (SEM, TEM, AFM, etc.) instruments [20]. These approaches offer several advantages over other characterization techniques. For example, these experiments are directly probing changes of the catalysts when the reaction is occurring and, thus, directly relevant information about the nature of active sites, intermediates, and spectators can be obtained. Although the list of technical possibilities is extensive, the most commonly utilized *operando* technique in catalysis is IR [20,21]. A typical experimental setup is shown in Figure 2 [21]. The key *operando* results conveyed in the sections below are obtained through XPS, XAS (XANES/EXAFS), Raman, STEM, and XRD techniques.

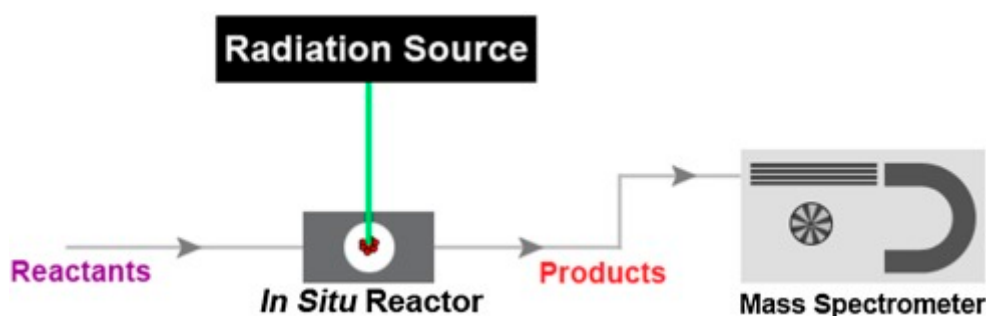


Figure 2. Schematic representation of a typical *in situ/operando* experimental setup. Figure reproduced with permission from [21].

3. Oxidative Dehydrogenation (ODH) of Light Alkanes (Ethane and Propane)

Ethylene and propylene are the most important chemical building blocks and their yearly worldwide demands increased at least 3.3% and 4.6%, respectively, in 2015 [22,23]. They are presently produced from a non-selective and energy intensive steam cracking process. An oxidative dehydrogenation process can produce these olefins at much lower temperatures (from 800 °C to 300–400 °C) with higher selectivity, with less waste and fewer separation steps. Ethane and propane are the most abundant components of shale gas after methane, and the ODH process offers an attractive route to upgrade them into more valuable olefins. This catalyst can catalyze the ODH reaction at mild conditions (0–35 atm and 250–450 °C) with promising results (45%–65% conversion and >90% selectivity) [3,24].

The catalyst components undergo changes in oxidation states and concentration due to volatility upon exposure with varying amounts of reactants. The Mars-van-Kravelen mechanism has been identified to exist in most oxidation reactions [25,26]. It indicates that the oxygen dehydrogenating the alkane comes from lattice oxygen sites that are eventually replenished by gas phase oxygen [25,26]. Having a facile redox character, V is the main component whose oxidation state is most greatly affected by the reaction. The V^{+5} dimer in the M1 phase are considered to activate alkanes since the M2 phase does not contain the element Nb or V^{+5} sites [11,26]. As shown in Figure 3, the application of XPS along with oxygen plasma treatment indicates that ethane conversion is directly related to the ratio of V^{+5}/V^{+4} [27]. This change however does not affect the M1 phase structure. The tellurium mainly exists in the state of Te^{+4} with minor amounts of Te^{+6} and it does not undergo significant changes during the reaction. Its role is attributed to stabilizing the M1 phase [28]. However, in another XPS study, the formation of reduced $Te(0)$ aggregates that block the active sites was concluded to be the main reason for catalyst deactivation, whereas a low amount of Te is believed to induce the formation of other crystalline phases, such as (V, Nb)-substituted θ - Mo_5O_{14} and MoO_2 [29]. Therefore, catalysts with a high V content and a moderate amount of Te content are recommended [29].

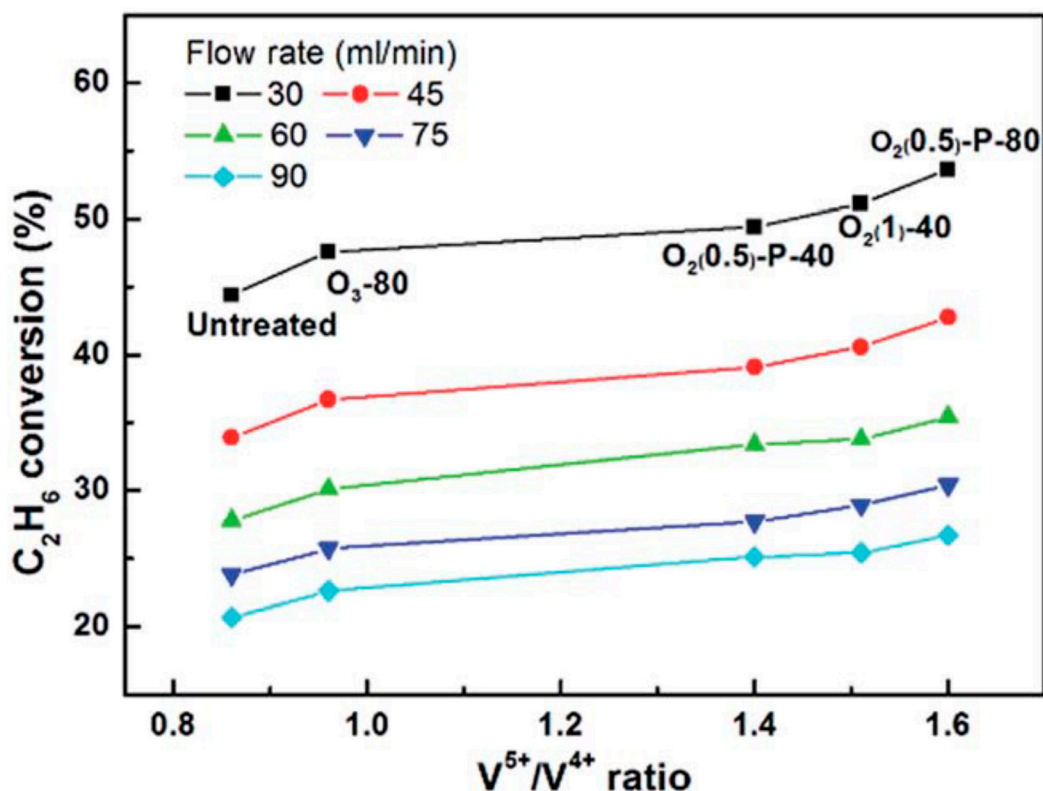


Figure 3. Ethane conversion as a function of V^{5+}/V^{4+} ratio as measured by XPS and oxygen plasma treatment. Reaction conditions: 400 °C, atmospheric pressure, $C_2H_6/O_2/He$ molar ratio = 30/20/50, $W/F_{C_2H_6}$ (W is the catalyst mass and $F_{C_2H_6}$ is the ethane molar flowrate) = 20.7–6.91 g_{cat} h mol C_2H_6 . Bulk compositions of catalysts, O₃-80 = MoV_{0.21}Te_{0.25}Nb_{0.09}, O₂ (0.5)-P-40 = MoV_{0.22}Te_{0.24}Nb_{0.09}, O₂ (1)-P-40 = MoV_{0.21}Te_{0.24}Nb_{0.09}, and O₂ (0.5)-P-80 = MoV_{0.21}Te_{0.22}Nb_{0.08}. Figure reproduced with permission from [27].

The same authors also suggested that addition of nanosized CeO₂ to the M1 phase improves the catalyst activity [28]. Due to its unique redox properties, CeO₂ is an excellent oxygen storage material which can consequently increase the abundance of V^{5+} on the catalyst surface [30]. A similar improvement in ethylene yield is achieved by Ishchenko et al. with Bi-doped M1 samples, which increases the surface V^{5+}/V^{4+} ratios [31]. In another XPS study by Nguyen et al., the surface V^{5+} content is claimed to be directly related to the total bulk V content [32]. This V^{5+} concentration is directly proportional to ethane conversion to a certain level of V in the catalyst. However, since there is a maximum level of activity for a given V content in the M1 unit cell, a very high V content might reduce reactivity [32]. The addition of SiO₂ decreases the agglomeration and sintering of the M1 phase crystals, increasing conversion without an effect on selectivity. A heat treatment under nitrogen at 870 K decreases conversion with an increase in selectivity due to a decrease of small pores where complete oxidation takes place [33].

The effect of substitution of Te by Sb in MoVTe(Sb)NbO_x catalysts was analyzed by Deniau et al. using *in situ* XANES and XPS [34]. After reduction by propane, no change in the V spectrum was observed, whereas the presence of Te⁺² (5%) was detected. These Te⁺² sites, which are also detected by XPS in larger amounts, may further be reduced to volatile Te (0). Therefore, the surface content of Te would depend on redox atmosphere under the reaction conditions. In the case of Sb, 15% of Sb⁺⁵ were reduced under similar conditions. Sb and Te affect the selectivity only in the case of propane, and not ethane, indicating that they may not be directly involved in dehydrogenation of alkanes, but in subsequent transformation of intermediates [34]. Contrarily, Te-free catalysts having Sb₄Mo₁₀O₃₁ and Mo_xM_{1-x}O_{2.8} ($M = V$ or Nb) are claimed by Solsona et al. and Xie et al.

separately to reduce ethylene selectivity [35,36]. The major drawback of Te-containing catalysts are their volatility and, consequently, substitution of Te with Sb or Bi is recommended from the point of view of future industrialization [34]. The incorporation of Te causes the formation of active and selective Te-containing phases, such as $\text{Te}_2\text{M}_{20}\text{O}_{57}$ ($\text{M} = \text{Mo}, \text{V}, \text{Nb}$), and prevent the formation of nonselective MoO_2 crystals [37]. Raman spectroscopy indicated the MoO_2 phase development as the reaction temperature is raised [38]. In another combined XAS and electrical conductivity *operando* study by Safonova et al., changes in oxidation states of Sb and V occur simultaneously with the same kinetics [39]. The M1 phase is described to be of the n^- semiconductor type. Its hexagonal channels serve as oxygen reservoirs and conductance has a direct relationship with changes in oxidation states of Sb and V [39].

Another factor impacting reactivity is the exposed morphology of the MoVTeNbO_x catalysts. Combination of STEM with He ion microscopy (HIM) images, Rietveld analysis and kinetic test studies by Melzer et al. indicate that ethane ODH reactivity is related to availability of (001), (120), and (210) facets at the surface of M1 crystals [40]. The low activity of the (010) facet is due to the formation of stable M_6O_{21} units. Therefore, the differences in activity among M1 samples of equal composition are due to the morphology of the particles which determines the terminating facets [40]. From high-resolution TEM and energy-dispersive X-ray techniques, Valente et al. reported that tellurium departure preferentially occurs from the end sides of the M1 crystals, across the (001) plane, even causing the destruction of the M1 phase [38]. As shown in Figure 4, this Te volatilization with MoO_2 formation causes a decrease in reactivity. In a recent *in situ* environmental STEM-(HA)ADF study by Aouine et al., the role of hexagonal channels as oxygen reservoirs, and the involvement of Te-O_x chains the redox bulk process have been reported [41]. The removal or diffusion of labile oxygen in the chains, does not require the reduction of Te^{+4} and, thus, reduction of Mo or V could be inferred [39]. This leads to another conclusion that reduction is not limited to the surface, but also involves hexagonal channels. All images along the (001) axis indicate the presence of $\{\text{Mo}(\text{Mo})_5\}$ terminating structural units linked to each other and, thus, structurally-active sites are not exposed on these facets [41].

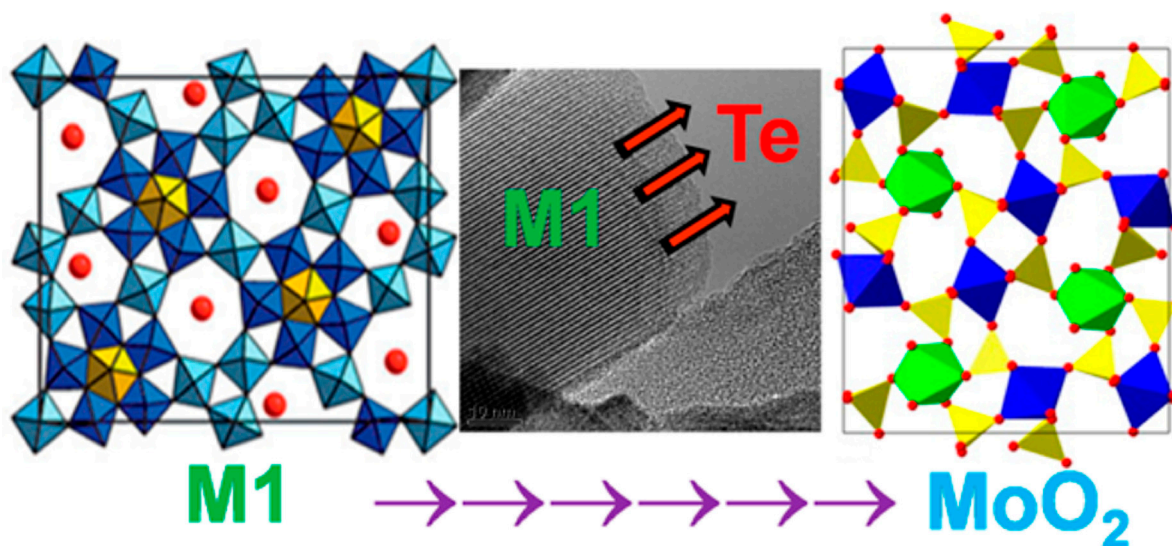


Figure 4. Destruction of the M1 phase through departure of metallic tellurium (Te^0) and formation of MoO_2 crystals at reaction temperatures of $\geq 500^\circ\text{C}$ which results in loss of ODH activity. Red corresponds to Te, yellow to NbO_7 , blue to MoO_6 , and light blue to MO_6 , occupied by both Mo and V cations. Figure reproduced with permission from [38].

4. Propane Ammoxidation to Acrylonitrile

Acrylonitrile, C_3H_3N , which is a monomer used to make several important polymers, is currently produced by ammoxidation of propylene (with ammonia and air) using bismuth phosphomolybdate catalysts in the SOHIO process [42,43]. Its production capacity is ~5.5 billion kg per year worldwide [44]. It is highly desirable to replace propylene with propane since the former is almost twice as expensive due to limited supply [44]. Several catalyst systems, such as Al-Sb-V-W-O, Ga-Sb-Ni-P-W-O/SiO₂, etc. have been reported in the literature [45–47]. The most promising systems reported so far are MoVNbTeO_x and MoVNbSbO_x catalysts, giving acrylonitrile yields of 62% and 55%, respectively, at moderate reaction conditions (<450 °C and 1–15 atm) [7,11,48–51].

The M2 phase, by itself, is incapable of activating propane due to its lack of V⁺⁵ sites [50]. However, the presence of M2 phase in the catalytic system is found to improve acrylonitrile selectivity [15,50], although a recent study by Woo et al. suggested the M1 phase is the only phase required for both the activity and selectivity in propane ammoxidation [52]. The STEM microscopy approach has been adopted to analyze the synergetic effects of this M1/M2 mixture [15,51]. Tellurium sites in hexagonal channels of both M1 and M2 phases are toward V-occupied framework sites, whereas these Te sites in the heptagonal channel of M1 are near the channel center [9]. EPR was then employed to confirm the presence of V⁺⁴ and Mo⁺⁵ in M1 and V⁺⁴ in M2. He et al. reported that M₆O₂₁ units in the M1 phase form different types of interfaces with the M2 phase and stressed the importance of controlling the mixing of these two phases [15]. High-resolution TEM studies indicated that the M1 phase domain decreases in the order: Mo-V-Te-Nb-O > Mo-V-Te-O > Mo-V-O. Therefore, Nb and Te are claimed to play a stabilizing role [53]. In a paper by Shiju et al., modeling was done to fit the experimental XRD data. Mo-V-Te-O and Mo-V-O M1 phases were claimed to have a similar orthorhombic unit cell to that of the Mo-V-Te-Nb-O M1 phase [54]. The presence of Nb pentagonal bipyramidal sites increases the redox behavior, which could explain the trend of acrylonitrile selectivity during propane ammoxidation: Mo-V-O < Mo-V-Te-O < Mo-V-Te-Nb-O [54].

Gulians et al. employed the surface sensitive low-energy ion scattering (LEIS) after methanol and allyl alcohol adsorption and reached the conclusion that surface TeO_x and NbO_x sites are unable to chemisorb these probe molecules to the same extent as the MoO_x and VO_x sites [55]. The different catalytic behaviors of these sites in Mo-V-O and Mo-V-Te-Nb-O systems can be attributed to the different locations of V⁺⁵ sites [55]. DFT studies, however, indicate that the reduced Mo is the most favorable site for ammonia activation [56], whereas Te is more active than V for the H abstraction from propane [57].

The role of Nb was studied by Desanto et al. using selected area electron diffraction (SAED) experiments with MoVTaTeO and MoVNbTeO catalysts [58]. The substitution effect of Ta was explained by the fact that Ta, unlike Nb, is clearly distinguishable from other metals during scattering experiments [58]. Ta⁺⁵ sites occupy pentagonal bipyramid centers similar to Nb⁺⁵. The indirect role of Nb⁺⁵ was claimed to increase the number of acidic Mo⁺⁶ sites, thereby increasing acrylonitrile selectivity. The higher conversion of MoVTaTeO catalyst stems from an increase in the concentration of active sites per surface area [58]. In their earlier paper, TEM, synchrotron X-ray powder diffraction (S-XPD), and neutron powder diffraction (NPD), were used to reach the conclusion that V⁺⁵-O-V⁺⁴/Mo⁺⁵ moieties adjacent to Te⁺⁴ and Mo⁺⁶ sites in the (001) terminal plane provide a spatially-isolated active site at which the selective ammoxidation of propane occurs [59]. Another factor impacting catalysis is the location of these sites. In one study, atomic layer deposition with alumina was employed to passivate the *ab* planes [60]. These passivated catalysts show very low conversion (<15%) with almost >95% selectivity to CO_x, compared to catalysts where the *ab* planes are exposed where propane conversion of 40%–65% and acrylonitrile selectivity of 50%–70% were achieved [60]. These results indicate the highly selective nature of the *ab* planes.

Raman, IR, and XRD were employed by Popova et al. to analyze the effect of preparation on phase composition. They concluded that the sample synthesized by spray drying is active and selective due to the presence of both orthorhombic M1 and hexagonal M2, whereas the activity of the sample made

by heat evaporation is low since it only contains hexagonal M2, $\text{TeMo}_5\text{O}_{16}$, and $\text{Mo}_{5-x}(\text{V}/\text{Nb})_x\text{O}_{14}$ phases [61]. The different mechanism of phase formation is attributed to the different chemical nature of precursors used in each method. XPS was used to indicate the higher Te^{+4} concentrations in the Ce-promoted the $\text{MoV}_{0.3}\text{Te}_{0.23}\text{Nb}_{0.24}$ mixed oxide (M) catalyst [62]. As in the case of oxidative dehydrogenation of alkanes [28], the presence of $\text{Ce}^{+3}/\text{Ce}^{+4}$ pairs is claimed to promote the redox ability of V and Mo sites on the catalyst [62].

Baca et al. utilized XANES, ESR, XPS, and Mossbauer spectroscopic techniques to examine the oxidation states of the various cations in the $\text{MoVTe}(\text{Sb})\text{NbO}$ catalysts for propane ammoxidation [63]. Tellurium and niobium mainly exist as fully oxidized Te^{+4} and Nb^{+5} whereas molybdenum, vanadium, and antimony are present as Mo^{+4} and Mo^{+5} , V^{+4} and V^{+5} , and Sb^{+3} and Sb^{+5} pairs, respectively. The characterization of the catalysts after propane ammoxidation showed very few changes in structures and compositions. Oxygen may be stored in the hexagonal channels and the mobility of these oxygen species only bound to Sb or Te cations should be high [63]. Such a property is not easy to monitor since the stoichiometries of oxygen, tellurium, and antimony can vary in the channels. In an *in situ* XANES by Shiju et al. for MoVNbTeO_x catalysts, the same oxidation states are reported in the bulk M1 phase. Nb, Te, and Mo did not undergo changes in oxidation states under the redox conditions employed but V produced changes in XANES spectra (unlike the study by Baca et al.), leading the conclusion that VO_x sites are the active species [64]. These results highlight the need for a greater experimental emphasis on the nature of active oxygen species and their role in the reaction mechanism. In terms of hydrocarbon intermediates, ^{13}C NMR was employed by Shiju et al. with ^{13}C labeled propane to study the possible presence of C6-intermediates during the course of the propane ammoxidation reaction. The labeling patterns in the final products exclude C6-intermediates, such as hexadiene [65].

5. Selective Oxidation of Propane to Acrylic Acid

Acrylic acid, $\text{C}_3\text{H}_4\text{O}_2$, with an annual production of 4.7 million tons, is a very important chemical intermediate with a major application in surface coatings, and its global market size is estimated to reach \$13 billion USD by 2020 [66,67]. It is currently produced in a two-step process with the oxidation of propylene to acrolein, subsequently followed by oxidation to acrylic acid [68]. Due to the rising demand of propylene for other purposes, it is advantageous to have an alternative process that can directly produce acrylic acid from propane in a single step. Among all of the catalysts reported to date for this process [69–71], $\text{MoVTe}(\text{Sb})\text{Nb}(\text{Ta})$ mixed metal oxides are the most promising, achieving acrylic acid yields of 50% [72]. However, this is still low compared to the current industrial two-step process with a yield of 80% [68]. Improvements in both catalyst structures/compositions and reactor conditions of this $\text{MoVTe}(\text{Sb})\text{Nb}(\text{Ta})$ catalyst system will complement additional cost savings from elimination of an additional step and, thus, further research is necessary to industrialize this new process.

Deniau et al. used Raman, XRD, XANES, and V NMR to study the effect of Ti, Sn, Ge, and W substitutions in the $\text{MoVTe}(\text{Sb})\text{NbO}$ catalysts [73]. V K-edge XANES spectra did not show the substitution effect, although Raman showed the presence of Keggin-type $(\text{GeMo}_{12}\text{O}_{40})^{4-}$ species in the Ge-promoted catalyst. The presence of Ge increased reactivity, while Ti and Si had an opposite effect. W did not have any positive or negative promotion effect. The effect of Ge which did not enter the M1 phase (based on XRD results) could be explained by the formation of new Ge containing species during catalyst synthesis, which led to an increase of V content of the M1 phase [73]. In another paper, the alkali (Na, K, etc.) doped catalysts activated at 600 °C present higher acrylic acid yields than the undoped catalysts due to the increase in surface area, the decrease in the number of acid sites and the stability of the crystalline phases during the catalyst activation [74].

The effect of steam on the electronic and surface structure of the MoVTeNbO_x catalyst was studied by Heine et al. using *operando* microwave conductivity, X-ray photoelectron, soft X-ray absorption, and resonant photoelectron spectroscopy under reaction conditions at 350 °C [66]. As shown in Figure 5,

steam increases both activity and acrylic acid selectivity. This result is explained by the fact that steam causes the decrease of electrical conductivity, the increase of the concentration of V^{+5} and Te^{+6} and the decrease of Mo^{+6} on the surface. The catalyst can, therefore, be concluded to act like a semiconducting gas sensor where the bulk conductivity can be used to detect electronic changes on the surface [66].

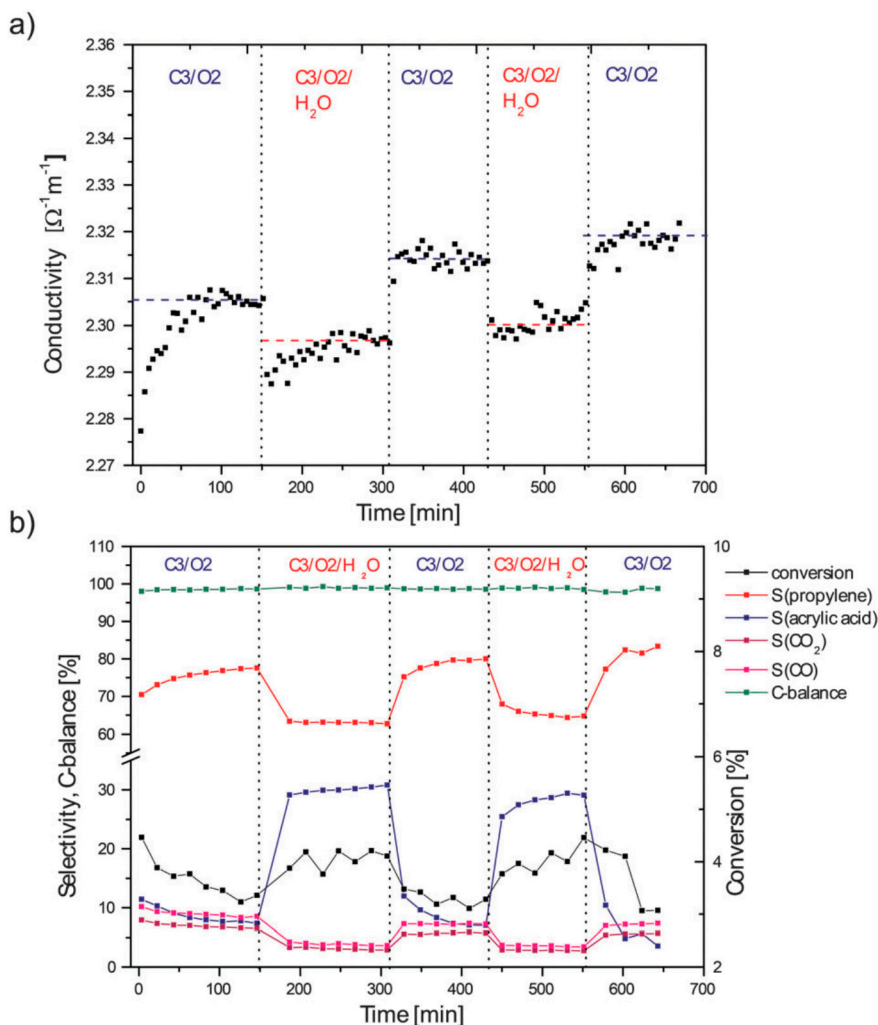


Figure 5. (a) *Operando* microwave conductivity measurements with and without steam at 350 °C and (b) simultaneously collected catalytic data. The catalyst had metal contents of 65 at % Mo, 6 at % Te, 19 at % V, and 10 at % Nb. The experiment was performed under wet and dry feed conditions containing 3 vol % propane, 6 vol % oxygen, and 5 vol % steam for the wet feed with residual N₂ gas at 350 °C. Figure reproduced with permission from [66].

Extensive *in situ/operando* XPS and XRD studies were performed by the same group in other papers to analyze the surface and bulk catalyst compositions/structures during the propane oxidation reaction [17,75,76]. *In situ* XPS indicates that the yield of acrylic acid increases with decreasing amount of Mo and increasing molar ratio of Te/V (V^{+5} oxo-species in close vicinity to Te^{+4} sites) at the surface. The mobility of Te in the presence of water vapor (steam) causes the enhanced selectivity to acrylic acid [17,75]. Adsorption of propane after catalysis shows a decrease of the heat of adsorption, which implies that the surface is restructured during the reaction [17]. This surface restructuring also indicates that active sites do not contain all the elements of the M1 phase and the surface composition of the M1 phase differs greatly from the bulk. The catalyst surface changes dynamically and reversibly with variations in feed compositions, but only in the outermost surface layer to a depth of around one nanometer [76]. The active sites are, therefore, proposed to be embedded in a thin surface layer

enriched in V, Te, and Nb, but depleted in Mo, as presented in Figure 6 [17]. This conclusion was later supported by *in situ* XRD studies which showed the remarkable stability of the bulk structure with no indication for segregation of any phases. However, the morphology of the M1 particles is damaged after prolonged periods due to reduction and evaporation of Te [76]. A debate remains in the literature surrounding the nature of the surface restructuring process and identifying the active species. From the *in situ* XPS data a hydrolysis-induced surface restructuring model was proposed that included the diffusion of Te oxo-species onto the lateral surfaces of the rod-like crystallites. Buttrey and coworkers emphasized that a polycrystalline material was used in this experiment and, hence, XPS will only offer an averaged surface composition. They contend that with only about 20% of the (001) surface exposed and 80% lateral surfaces, the XPS changes could also result from a process where water alters or removes amorphous species commonly associated with the more abundant lateral surfaces [77]. This comes from the observation that during crystal growth disordered appended octahedral and pentagonal ring units are associated with the lateral surfaces while the (001) plane (believed to be the active surface) remains clean [77]. This debate might be resolved if it were possible to grow a single crystal of the M1 phase of sufficient dimension to probe with angular resolved microscopy under *operando* conditions.

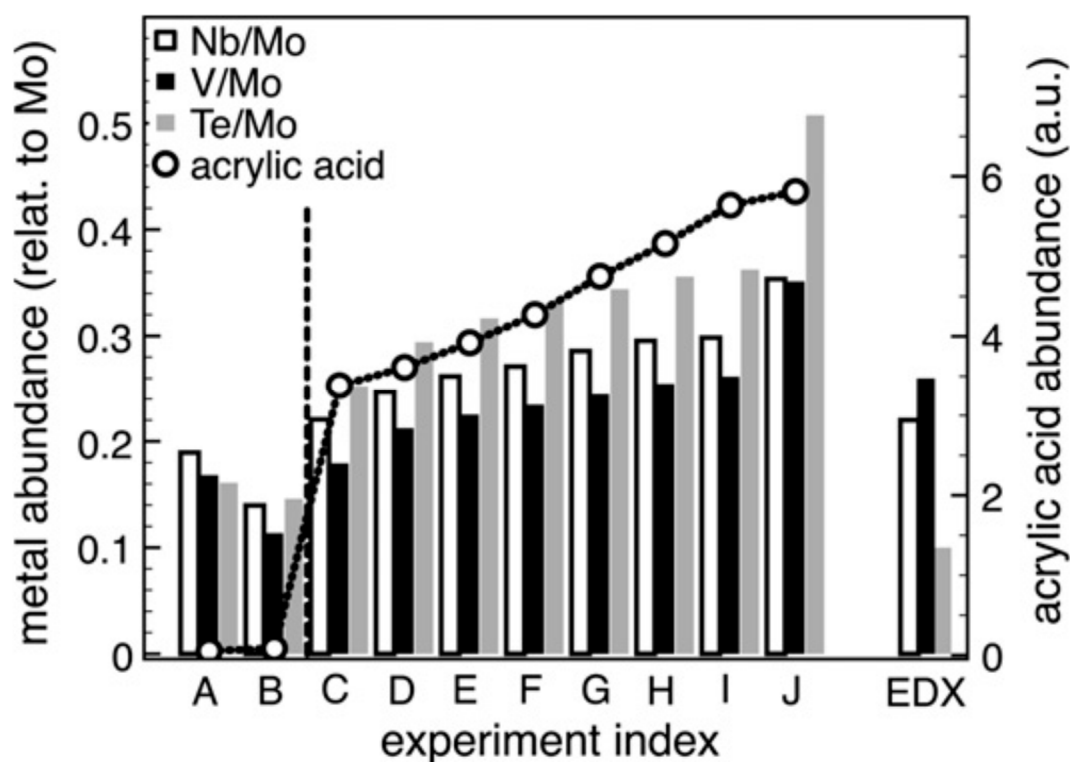


Figure 6. Elemental metal surface composition as determined by *operando* XPS with the simultaneously-recorded acrylic acid abundance. The $\text{MoV}_{0.27}\text{Te}_{0.10}\text{Nb}_{0.24}$ catalyst was used and the temperature was increased stepwise from 323 K (50 °C) to 513 K (240 °C), and finally to 693 K (420 °C) during *operando* XPS measurements. After approximately 10 h TOS in dry feed ($\text{C}_3\text{H}_8/\text{O}_2/\text{He} = 2/1/2.8$ sccm (measurements A and B)), steam has been added ($\text{C}_3\text{H}_8/\text{O}_2/\text{H}_2\text{O}(\text{g}) = 2/1/2.8$ sccm (measurements C–J)). The switch from dry to wet feed is indicated by the dashed vertical line. The bulk composition as obtained by EDX before the reaction is also shown for comparison. Figure reproduced with permission from [17].

In a study by Naraschewski et al. [12], the activity of the M1 phase is claimed to be independent of the total Te concentration although Te^{+4} is suggested to be active for α -H abstraction [50]. The role of surface Te was not characterized or mentioned in their paper [12]. The role of Nb was studied by

Concepcion et al. [14] and Zhang et al. [78]. Although the MoVTeO sample already has the M1 phase, the presence of Nb⁺⁵ ions in the MoVTeNbO samples decreases the number of acid sites, stabilizes the crystalline structures, and reduces further degradation of acrylic acid to carbon oxides (CO, CO₂, etc.), eventually resulting in much-improved acrylic acid yields [13,53,79]. Although the XRD patterns show the same M1 phase for MoVTeO and MoVTeNbO catalysts, Raman spectroscopy was able to detect the presence of NbO_x species whose presence decrease the strength of acidity as detected by the NH₃-TPD. Exchange rates with gas phase oxygen were analyzed by temperature-programmed ¹⁸O₂-experiments and the amount of exchangeable oxygen species in the Nb-containing catalysts is found to be higher than the corresponding Nb-free catalysts [14]. In addition, their XPS studies indicate that the MoVTeNbO catalysts have a higher concentration of Te⁺⁴ species (and no Te⁺⁶ species) than the MoVTeO catalyst, which also contain a detectable amount of Te⁺⁶ species. The *in situ* STEM and HR TEM images by Zhang et al. indicate the strong bonding and correlation between the (Mo,V)O₆ octahedra and the central Nb moieties in the pentagonal channels. Since these centers cannot be pre-made, they must be formed upon catalyst activation [78].

The importance of the (001) plane of the M1 phase of the MoVTeNb oxide catalyst was analyzed by Sanfiz et al. by preferentially exposing this surface through silylation [80]. Scanning electron microscopy and transmission electron microscopy, along with high-sensitivity low-energy ion scattering (HS-LEIS) methods, were used to characterize the catalysts. Their results indicated that the (001) plane does not have superior catalytic properties [80]. Further studies are needed to analyze the effect of other planes on reactivity/selectivity.

6. Discussion

In this complex mixed metal oxide system, crystal structures, surface composition, and oxidation states (redox potential) of components play crucial roles in reactivity and selectivity. Based on the Mars-van-Krevelen mechanism prevalent in these oxidation reactions, the role of lattice oxygen must be analyzed further to quantify their transport between the bulk and surface regions, as well as understand their role in selectivity [81]. The site isolation concept for oxidation catalysts is based on the idea that this reactive oxygen must be readily available while the rest of the structure acts as a control system for the electronic and physical properties of the catalysts [82]. In general, the demanding nature of these reactions might preclude the collapse of the fine structure over extended periods but a robust quality has been demonstrated through at least one example of redox cycling [83]. Stability with time-on-stream, as well as resistance to coking and poisoning, have not been widely addressed for this system and present excellent opportunities where *in situ* and *operando* studies can provide new insight.

Although a great volume of work has been conducted by researchers indicated in this review, and others, a central unifying concept is lacking for further catalyst development as to metals composition, surface heterogeneity, or active oxygen species. For example, V⁺⁵/V⁺⁴ pairs are claimed to be responsible for active lattice oxygen in most publications [11,25–27,50,76] but changes in oxidation states of Mo, Te(Sb), and Nb are debated based on techniques used (XPS vs. XANES/EXAFS, etc.) and the type of oxidation reactions [11,25,26]. In some studies, Te sites are concluded to contribute to the redox nature of V sites and steam aids the mobility of these Te species [17,41] with their full reduction causing deactivation [29,41] but, in another study, Te sites are concluded to be unaffected during experiments [64]. Similarly, Nb is claimed to contribute to oxygen exchange rates [14], although in other studies, its oxidation states are not affected [64], or its role is to only stabilize the M1 phase [13,64]. One additional factor to be considered is that the time of experiments by some researchers may not be long enough to observe significant changes. Even the presence of the M2 phase affecting selectivity in propane ammoxidation is not agreed upon [15,50,52]. The roles of active exposed planes during the reaction are also debated [77,80]. Careful characterization experiments with controlled structures/compositions need to be performed in order to resolve these issues. Such progress, however,

is hampered by the difficulty of (a) generating phase-pure materials and (b) growing well-defined single crystals of significant proportion.

The treatment of oxide catalysts as semiconductors where the bulk conductivity gives electronic information about the surface needs to be considered with caution since deeper subsurface lattice oxygen are claimed to generate different products from surface oxygen [83]. Modern depth profiling of *in situ/operando* approaches, such as XPS or LEIS, with isotope exchange experiments could shed some light in distinguishing these oxygen species. So far such experiments have only been performed in the selective oxidation of propane to acrylic acid reaction [17]. Applying micro-kinetic studies with controlled transport diffusion phenomena would be beneficial to determine how surface-adsorbed oxygen may react differently than species delivered through transport from the bulk [83]. Understanding micro-kinetic processes with respect to each metal component is crucial to relate its relevant role in the overall mechanism of the reaction.

Further studies are also needed to elucidate the overall mechanism of these oxidation reactions. The low oxygen reaction order indicates that the generation of activated oxygen is not involved in the kinetically-difficult step [81]. However, the rates with respect to different intermediate steps, C–H activation, C–C breaking, C–O formation, etc., are not yet systemically studied or known. *Operando/in situ* steady-state isotope-transient kinetic analysis (SSITKA) IR, TAP (temporal analysis of products), or NMR experiments with simultaneous monitoring of both intermediate and production formation could provide further information about these mechanistic steps. Along with these transient experiments, titration methods should be designed to count the number of active sites involving different reaction processes. The concept of special active sites is important since Sir H.S. Taylor proposed in 1925 that only a fraction of surface atoms are responsible for heterogeneous catalysis [84]. These transient methods are important in catalyst development in a sense that ‘the catalytic function is a transient property of the catalyst structure on its way to thermodynamic equilibrium’ [81]. These transient characterization experiments have not been greatly explored and may be able to derive the role of key promoters or unique compositions for mixed metal oxide catalysts with improved catalyst activity.

7. Summary and Outlook

Recent advances in the past 20 years through *in situ/operando* studies of the MoVTaNbO_x catalyst development for oxidation reactions are discussed in this review. Although the state-of-the-art *in situ/operando* techniques improve the understanding of these catalysts under relevant conditions, further progress is still necessary to replace the existing technology with the new industrial processes employing these catalysts. Deactivation studies, as well as insights from transient techniques, are also necessary to unravel the underlying phenomena of these selective oxidation catalysts. The topic of light alkane activation/oxidation is poised to take off in upcoming years due to the abundance of shale gas resources. From the advances in understanding summarized here through *in situ/operando* studies, it can be seen that an investment in such instrumentation, methodology, and analysis will greatly benefit the development of next-generation M1-based materials that demonstrate superior performance that may, in the future, supplant existing energy-intensive technologies.

Acknowledgments: This work was supported by the U.S. Department of Energy, under DOE Idaho Operations Office Contract DE-AC07-05ID14517. Accordingly, the U.S. Government retains a nonexclusive, royalty-free license to publish or reproduce the published form of this contribution, or allow others to do so, for U.S. Government purposes.

Author Contributions: All authors equally contributed to the manuscript.

Conflicts of Interest: The authors declare no conflict of interest.

References

1. Faramawy, S.; Zaki, T.; Sakr, A.A.-E. Natural gas origin, composition, and processing: A review. *J. Nat. Gas Sci. Eng.* **2016**, *34*, 34–54. [[CrossRef](#)]

2. Vedrine, J.C. Heterogeneous partial (amm) oxidation and oxidative dehydrogenation catalysis on mixed metal oxides. *Catalysts* **2016**, *6*, 22. [CrossRef]
3. Gartner, C.A.; van Veen, A.C.; Lercher, J.A. Oxidative dehydrogenation of ethane: Common principles and mechanistic aspects. *ChemCatChem* **2013**, *5*, 3196–3217. [CrossRef]
4. Shiju, N.R.; Guliyants, V.V. Recent developments in catalysis using nanostructured materials. *Appl. Catal. A Gen.* **2009**, *356*, 1–17. [CrossRef]
5. Hatano, M.; Kayo, A. Catalytic Conversion of Alkanes to Nitriles, and a Catalyst Therefor. U.S. Patent 5049692, 1991.
6. Ushikubo, T.; Nakamura, H.; Koyasu, Y.; Wajiki, S. Method for Producing an Unsaturated Carboxylic Acid. European Patent 0608838, 1994.
7. Grasselli, R.K.; Burrington, J.D.; Buttrey, D.J.; DeSanto, P.; Lugmair, C.G.; Volpe, A.F.; Weingand, T. Multifunctionality of active centers in (amm) oxidation catalysts: From Bi-Mo-O_x to Mo-V-Nb-(Te, Sb)-O_x. *Top. Catal.* **2003**, *23*, 5–22. [CrossRef]
8. Ueda, W.; Vitry, D.; Katou, T. Structural organization of catalytic functions in Mo-based oxides for propane selective oxidation. *Catal. Today* **2004**, *96*, 235–240. [CrossRef]
9. DeSanto, P.; Buttrey, D.J.; Grasselli, R.K.; Lugmair, C.G.; Volpe, A.F.; Toby, B.H.; Vogt, T. Structural aspects of the M1 and M2 phases in MoVNbTeO propane ammoxidation catalysts. *Z. Für Krist.* **2004**, *219*, 152–165. [CrossRef]
10. Aouine, M.; Dubois, J.L.; Millet, J.M.M. Crystal chemistry and phase composition of the MoVTeNbO catalysts for the ammoxidation of propane. *Chem. Commun.* **2001**, 1180–1181. [CrossRef]
11. Grasselli, R.K.; Buttrey, D.J.; DeSanto, P.; Burrington, J.D.; Lugmair, C.G.; Volpe, A.F.; Weingand, T. Active centers in Mo-V-Nb-Te-O_x (amm) oxidation catalysts. *Catal. Today* **2004**, *91–92*, 251–258. [CrossRef]
12. Naraschewski, F.N.; Kumar, C.P.; Jentys, A.; Lercher, J.A. Phase formation and selective oxidation of propane over MoVTeNbO_x catalysts with varying compositions. *Appl. Catal. A Gen.* **2011**, *391*, 63–69. [CrossRef]
13. Baca, M.; Pigamo, A.; Dubois, J.L.; Millet, J.M.M. Fourier transform infrared spectroscopic study of surface acidity by pyridine adsorption on the M1 active phase of the MoVTe(Sb)NbO catalysts used in propane oxidation. *Catal. Commun.* **2005**, *6*, 215–220. [CrossRef]
14. Concepcion, P.; Hernandez, S.; Lopez Nieto, J.M. On the nature of active sites in MoVTeO and MoVTeNbO catalysts: The influence of catalyst activation temperature. *Appl. Catal. A Gen.* **2011**, *391*, 92–101. [CrossRef]
15. He, Q.; Woo, J.; Belianinov, A.; Guliyants, V.V.; Borisevich, A.Y. Better catalysts through microscopy: Mesoscale M1/M2 intergrowth in molybdenum-vanadium based complex oxide catalysts for propane ammoxidation. *ACS Nano* **2015**, *9*, 3470–3478. [CrossRef] [PubMed]
16. Baca, M.; Aouine, M.; Dubois, J.L.; Millet, J.M.M. Synergetic effect between phases in MoVTe(Sb)NbO catalysts used for the oxidation of propane into acrylic acid. *J. Catal.* **2005**, *233*, 234–241. [CrossRef]
17. Havecker, A.; Wrabetz, S.; Krohnert, J.; Csepei, L.; Naumann, R.; Alnoncourt, D.; Kolen'ko, Y.V.; Girgsdies, F.; Schlögl, R.; Trunschke, A. Surface chemistry of phase-pure M1 MoVTeNb oxide during operation in selective oxidation of propane to acrylic acid. *J. Catal.* **2012**, *285*, 48–60. [CrossRef]
18. Grasselli, R.K.; Lugmair, C.G.; Volpe, A.F. Towards an understanding of the reaction pathways in propane ammoxidation based on the distribution of elements at the active centers of the M1 Phase of the MoV (Nb, Ta)TeO system. *Top. Catal.* **2011**, *54*, 595–604. [CrossRef]
19. Banares, M.A.; Guerrero-Perez, M.O.; Fierro, J.L.G.; Cortez, G.G. Raman spectroscopy during catalytic operations with on-line activity measurement (*operando* spectroscopy): A method for understanding the active centers of cations supported on porous materials. *J. Mater. Chem.* **2002**, *12*, 3337–3342. [CrossRef]
20. Weckhuysen, B.M. Determining the active site in a catalytic process: *Operando* spectroscopy is more than a buzzword. *Phys. Chem. Chem. Phys.* **2003**, *5*, 4351–4360. [CrossRef]
21. Chakrabarti, A.; Ford, M.E.; Gregory, D.; Hu, R.; Keturakis, C.J.; Lwin, S.; Tang, Y.; Yang, Z.; Zhu, M.; Banares, M.A.; Wachs, I.E. A decade + of *operando* spectroscopy studies. *Catal. Today* **2017**, *283*, 27–53. [CrossRef]
22. Global Ethylene Demand to Grow 3.3% Annually. Available online: <http://www.woodmac.com/analysis/11966725> (accessed on 4 August 2016).
23. Chemical Economics Handbook: Propylene. Available online: <https://www.ihs.com/products/propylene-chemical-economics-handbook.html> (accessed on 4 August 2016).

24. Arnold, S.C.; Gaffney, A.M.; Song, R.; Yeh, C.Y. Process for Producing Ethylene Via Oxidative Dehydrogenation (ODH) of Ethane. U.S. Patent 0256432, 2010.
25. Che-Galicia, G.; Quintana-Solorzano, R.; Ruiz-Martinez, R.S.; Valente, J.S.; Castillo-Araiza, C.O. Kinetic modeling of the oxidative dehydrogenation of ethane to ethylene over a MoVTeNbO catalytic system. *Chem. Eng. J.* **2014**, *252*, 75–88. [[CrossRef](#)]
26. Schlögl, R. Active sites for propane oxidation: Some generic considerations. *Top. Catal.* **2011**, *54*, 627–638. [[CrossRef](#)]
27. Chen, X.; Yang, Q.; Chu, B.; An, H.; Cheng, Y. Valence variation of phase-pure M1 MoVNbTe oxide by plasma treatment for improved catalytic performance in oxidative dehydrogenation of ethane. *RSC Adv.* **2015**, *5*, 91295–91301. [[CrossRef](#)]
28. Chu, B.; An, H.; Nijhuis, T.A.; Schouten, J.C.; Cheng, Y. A self-redox pure-phase M1 MoVNbTeO_x/CeO₂ nanocomposite as a highly active catalyst for oxidative dehydrogenation of ethane. *J. Catal.* **2015**, *329*, 471–478. [[CrossRef](#)]
29. Chu, B.; Truter, L.; Nijhuis, T.A.; Cheng, Y. Performance of phase-pure M1 MoVNbTeO_x catalysts by hydrothermal synthesis with different post-treatments for the oxidative dehydrogenation of ethane. *Appl. Catal. A Gen.* **2015**, *498*, 99–106. [[CrossRef](#)]
30. Fan, J.; Wu, X.; Wu, X.; Liang, Q.; Ran, R.; Weng, D. Thermal ageing of Pt on low-surface-area CeO₂–ZrO₂–La₂O₃ mixed oxides: Effect on the OSC performance. *Appl. Catal. B Environ.* **2008**, *81*, 38–48. [[CrossRef](#)]
31. Ishchenko, E.V.; Kardash, T.Y.; Gulyaev, R.V.; Ishchenko, A.V.; Sobolev, V.I.; Bondareva, V.M. Effect of K and Bi doping on the M1 phase in MoVTeNbO catalysts for ethane oxidative conversion to ethylene. *Appl. Catal. A Gen.* **2016**, *514*, 1–13. [[CrossRef](#)]
32. Nguyen, T.T.; Deniau, B.; Delichere, P.; Millet, J.M.M. Influence of the content and distribution of vanadium in the M1 phase of the MoVTe(Sb)NbO catalysts on their catalytic properties in light alkanes oxidation. *Top. Catal.* **2014**, *57*, 1152–1162. [[CrossRef](#)]
33. Nguyen, T.T.; Aouine, M.; Millet, J.M.M. Optimizing the efficiency of MoVTeNbO catalysts for ethane oxidative dehydrogenation to ethylene. *Catal. Commun.* **2012**, *21*, 22–26. [[CrossRef](#)]
34. Deniau, B.; Nguyen, T.T.; Delichere, P.; Safonova, O.; Millet, J.M. Redox state dynamics at the surface of MoVTe(Sb)NbO M1 phase in selective oxidation of light alkanes. *Top. Catal.* **2013**, *56*, 1952–1962. [[CrossRef](#)]
35. Solsona, B.; Vazquez, M.I.; Ivars, F.; Dejoz, A.; Concepcion, P.; Lopez, J.M. Selective oxidation of propane and ethane on diluted Mo–V–Nb–Te mixed-oxide catalysts. *J. Catal.* **2007**, *252*, 271–280. [[CrossRef](#)]
36. Xie, Q.; Chen, L.; Weng, W.; Wan, H. Preparation of MoVTe (Sb) Nb mixed oxide catalysts using a slurry method for selective oxidative dehydrogenation of ethane. *J. Mol. Catal. A Chem.* **2005**, *240*, 191–196. [[CrossRef](#)]
37. Botella, P.; Garcia-Gonzalez, E.; Dejoz, A.; Lopez Nieto, J.M.; Vazquez, M.I.; Gonzalez-Calbet, J. Selective oxidative dehydrogenation of ethane on MoVTeNbO mixed metal oxide catalysts. *J. Catal.* **2004**, *225*, 428–438. [[CrossRef](#)]
38. Valente, J.S.; Armendariz-Herrera, H.; Quintana-Solorzano, R.; del Angel, P.; Nava, N.; Masso, A.; Lopez Nieto, J.M. Chemical, structural, and morphological changes of a MoVTeNb catalyst during oxidative dehydrogenation of ethane. *ACS Catal.* **2014**, *4*, 1292–1301. [[CrossRef](#)]
39. Safonova, O.V.; Deniau, B.; Millet, J.M. Mechanism of the oxidation-reduction of the MoVSbNbO catalyst: In *operando* X-ray absorption spectroscopy and electrical conductivity measurements. *J. Phys. Chem. B* **2006**, *110*, 23962–23967. [[CrossRef](#)] [[PubMed](#)]
40. Melzer, D.; Xu, P.; Hartmann, D.; Zhu, Y.; Browning, N.D.; Sanchez-Sanchez, M.; Lercher, J.A. Atomic-scale determination of active facets on the MoVTeNb oxide M1 phase and their intrinsic catalytic activity for ethane oxidative dehydrogenation. *Angew. Chem. Int. Ed.* **2016**, *55*, 8873–8877. [[CrossRef](#)] [[PubMed](#)]
41. Aouine, M.; Epicier, T.; Millet, J.M. In situ environmental STEM study of the MoVTe oxide M1 phase catalysts for ethane oxidative dehydrogenation. *ACS Catal.* **2016**, *6*, 4775–4781. [[CrossRef](#)]
42. *Handbook of Heterogeneous Catalysis*; Ertl, G.; Knozinger, H.; Weitkamp, J. (Eds.) Wiley/VHC: New York, NY, USA, 1997; pp. 2302–2326.
43. Grasselli, R.K. Advances and future trends in selective oxidation and ammoxidation catalysis. *Catal. Today* **1999**, *49*, 141–153. [[CrossRef](#)]

44. Holmberg, J.; Grasselli, R.K.; Andersson, A. Catalytic behavior of M1, M2, and M1/M2 physical mixtures of the Mo-V-Nb-Te-oxide system in propane and propene ammoxidation. *Appl. Catal. A Gen.* **2004**, *270*, 121–134. [[CrossRef](#)]
45. Guttman, A.T.; Grasselli, R.K.; Bradzil, J.F. Ammoxidation of Paraffins and Catalysts Therefor. U.S. Patent 4746641, 1988.
46. Nilsson, J.; Landa-Canovas, A.R.; Hansen, S.; Andersson, A. An investigation of the Al-Sb-V-W-Oxide system for propane ammoxidation. *J. Catal.* **1999**, *186*, 442–457. [[CrossRef](#)]
47. Zenkovets, G.A.; Kryukova, G.N.; Tsybulya, S.V.; Anufrienko, V.F.; Larina, T.V.; Burgina, E.B. The structure of oxide Ga-Sb-Ni-P-W-O/SiO₂ catalyst and its catalytic properties in propane ammoxidation. *Kinet. Catal.* **2002**, *43*, 384–390. [[CrossRef](#)]
48. Ushikubo, T.; Oshima, K.; Kayo, A.; Umezawa, T.; Kiyono, K.; Sawaki, I. Process for Producing Nitriles. European Patent 529853, 1992.
49. Komada, S.; Hinago, H.; Kaneta, M.; Watanabe, M. Process Using Niobium-Containing Aqueous Solution in Producing Niobium-Containing Oxide Catalyst. European Patent 0859809, 1998.
50. Grasselli, R.K. Selectivity issues in (amm) oxidation catalysis. *Catal. Today* **2005**, *99*, 23–31. [[CrossRef](#)]
51. Pyrz, W.D.; Blom, D.A.; Vogt, T.; Buttrey, D.J. Direct imaging of the MoVTaNbO M1 phase using an aberration-corrected high-resolution scanning transmission electron microscope. *Angew. Chem. Int. Ed.* **2008**, *47*, 2788–2791. [[CrossRef](#)] [[PubMed](#)]
52. Woo, J.; Sanghavi, U.; Vonderheide, A.; Guliants, V.V. A study of M1/M2 phase synergy in the MoVTe(Nb,Ta)O catalysts for propane ammoxidation to acrylonitrile. *Appl. Catal. A Gen.* **2016**, *515*, 179–189. [[CrossRef](#)]
53. Korovchenko, P.; Shiju, N.R.; Dozier, A.K.; Graham, U.M.; Guerrero-Perez, M.O.; Guliants, V.V. M1 to M2 phase transformation and phase cooperation in bulk mixed metal Mo-V-M-O (M = Te, Nb) catalysts for selective ammoxidation of propane. *Top. Catal.* **2008**, *50*, 43–51. [[CrossRef](#)]
54. Shiju, N.R.; Guliants, V.V.; Overbury, S.H.; Rondinone, A.J. Toward environmentally benign oxidations: Bulk mixed Mo-V-(Te-Nb)-O M1 phase catalysts for the selective ammoxidation of propane. *ChemSusChem* **2008**, *1*, 519–523. [[CrossRef](#)] [[PubMed](#)]
55. Guliants, V.V.; Brongersma, H.H.; Knoester, A.; Gaffney, A.M.; Han, S. Surface active sites present in the orthorhombic M1 phases: Low energy ion scattering study of methanol and allyl alcohol chemisorption over Mo-V-Te-Nb-O and Mo-V-O catalysts. *Top. Catal.* **2006**, *38*, 41–50. [[CrossRef](#)]
56. Yu, J.; Xu, Y.; Guliants, V.V. Propane ammoxidation over Mo-V-Te-Nb-O M1 phase investigated by DFT: Elementary steps of ammonia adsorption, activation and NH insertion into π -allyl intermediate. *Top. Catal.* **2014**, *57*, 1145–1151. [[CrossRef](#)]
57. Yu, J.; Xu, Y.; Guliants, V.V. Propane ammoxidation over Mo-V-Te-Nb-O M1 phase: Density functional theory study of propane oxidative dehydrogenation steps. *Catal. Today* **2014**, *238*, 28–34. [[CrossRef](#)]
58. DeSanto, P.; Buttrey, D.J.; Grasselli, R.K.; Pyrz, W.D.; Lugmair, C.G.; Volpe, A.F., Jr.; Vogt, T.; Toby, B.H. Comparison of MoVTaTeO and MoVNbTeO M1 crystal chemistry. *Top. Catal.* **2006**, *38*, 31–40. [[CrossRef](#)]
59. DeSanto, P.; Buttrey, D.J.; Grasselli, R.K.; Lugmair, C.G.; Volpe, A.F.; Toby, B.H.; Vogt, T. Structural characterization of the orthorhombic phase M1 in MoVNbTeO propane ammoxidation catalyst. *Top. Catal.* **2003**, *23*, 23–38. [[CrossRef](#)]
60. Shiju, N.R.; Liang, X.; Weimer, A.W.; Liang, C.; Dai, S.; Guliants, V.V. The role of surface basal planes of layered mixed metal oxides in selective transformation of lower alkanes: Propane ammoxidation over surface ab planes of Mo-V-Te-Nb-O M1 phase. *J. Am. Chem. Soc.* **2008**, *130*, 5850–5851. [[CrossRef](#)] [[PubMed](#)]
61. Popova, G.Y.; Andrushkevich, T.V.; Chesalov, Y.A.; Plyasova, L.M.; Dovlitova, L.S.; Ischenko, E.V.; Aleshina, G.I.; Khramov, M.I. Formation of active phases in MoVTaNb oxide catalysts for ammoxidation of propane. *Catal. Today* **2009**, *144*, 312–317. [[CrossRef](#)]
62. Wang, G.; Guo, Y.; Lu, G. Promotional effect of cerium on Mo-V-Te-Nb mixed oxide catalyst for ammoxidation of propane to acrylonitrile. *Fuel Process. Technol.* **2015**, *130*, 71–77. [[CrossRef](#)]
63. Baca, M.; Millet, J.M. Bulk oxidation state of the different cationic elements in the MoVTe(Sb)NbO catalysts for oxidation or ammoxidation of propane. *Appl. Catal. A Gen.* **2005**, *279*, 67–77. [[CrossRef](#)]
64. Shiju, N.R.; Rondinone, A.J.; Mullins, D.R.; Schwartz, V.; Overbury, S.H.; Guliants, V.V. XANES study of hydrothermal Mo-V-based mixed oxide M1-phase catalysts for the (amm) oxidation of propane. *Chem. Mater.* **2008**, *20*, 6611–6616. [[CrossRef](#)]

65. Shiju, N.R.; Kale, R.R.; Iyer, S.S.; Gulianti, V.V. ^{13}C isotope labeling study of propane ammoxidation over M1 phase Mo-V-Te-Nb-O mixed oxide catalyst. *J. Phys. Chem. C* **2007**, *111*, 18001–18003. [CrossRef]
66. Heine, C.; Havecker, M.; Trunschke, A.; Schlogl, R.; Eichelbaum, M. The impact of steam on the electronic structure of the selective propane oxidation catalyst MoVTeNb oxide (orthorhombic M1 phase). *Phys. Chem. Chem. Phys.* **2015**, *17*, 8983–8993. [CrossRef] [PubMed]
67. Acrylic acid market worth 13.21 billion USD by 2020. Available online: <http://www.marketsandmarkets.com/PressReleases/acrylic-acid.asp> (accessed on 7 August 2016).
68. Cavani, F. Catalytic selective oxidation: The forefront in the challenge for a more sustainable chemical industry. *Catal. Today* **2010**, *157*, 8–15. [CrossRef]
69. Novakova, E.K.; Vedrine, V.C. *Metal Oxides, Chemistry and Applications*; Fierro, J.L.G., Ed.; CRC Press: New York, NY, USA, 2006; pp. 414–416.
70. Centi, G.; Cavani, F.; Trifiro, F. *Selective Oxidation by Heterogeneous Catalysis*; Kluwer Academic/Plenum Publishers: New York, NY, USA, 2001; pp. 363–364.
71. Lin, M.M. Selective oxidation of propane to acrylic acid with molecular oxygen. *Appl. Catal. A* **2001**, *207*, 1–16. [CrossRef]
72. Ushikubo, T.; Nakamura, H.; Koyasu, Y.; Wajiki, S. Method for Producing an Unsaturated Carboxylic Acid. U.S. Patent 5380933, 1995.
73. Deniau, B.; Millet, J.M.M.; Loridant, S.; Christin, N.; Dubois, J.L. Effect of several cationic substitutions in the M1 active phase of the MoVTeNbO catalysts used for the oxidation of propane to acrylic acid. *J. Catal.* **2008**, *260*, 30–36. [CrossRef]
74. Ivars, F.; Solsona, B.; Botella, P.; Soriano, M.D.; Lopez Nieto, J.M. Selective oxidation of propane over alkali-doped Mo-V-Sb-O catalysts. *Catal. Today* **2009**, *141*, 294–299. [CrossRef]
75. Sanfiz, A.C.; Hansen, T.W.; Teschner, D.; Schnorch, P.; Girgsdies, F.; Trunschke, A.; Schlogl, R.; Looi, M.H.; Hamid, S.B.A. Dynamics of the MoVTeNb oxide M1 phase in propane oxidation. *J. Phys. Chem. C* **2010**, *114*, 1912–1921. [CrossRef]
76. D'Alnoncourt, R.N.; Csepei, L.; Havecker, M.; Girgsdies, F.; Schuster, M.E.; Schlogl, R.; Trunschke, A. The reaction network in propane oxidation over phase-pure MoVTeNb M1 oxide catalysts. *J. Catal.* **2014**, *311*, 369–385. [CrossRef]
77. Blom, D.; Vogt, T.; Allard, L.; Buttrey, D. Observation of sublattice disordering of the catalytic sites in a complex Mo-V-Nb-Te-O oxidation catalyst using high temperature STEM imaging. *Top. Catal.* **2014**, *57*, 1138–1144. [CrossRef]
78. Zhang, W.; Zhang, B.; Zheng, W.; Su, D.S. Electron-irradiation-stimulated atomic-scale structural dynamics of the pentagonal channel in a complex MoVTeNbO_x catalyst. *ChemCatChem* **2015**, *7*, 3651–3654. [CrossRef]
79. Ueda, W.; Vitry, D.; Katou, T. Crystalline Mo-V-O based complex oxides as selective oxidation catalysts of propane. *Catal. Today* **2005**, *99*, 43–49. [CrossRef]
80. Sanfiz, A.C.; Hansen, T.W.; Sakthivel, A.; Trunschke, A.; Schlogl, R.; Knoester, A.; Brongersma, H.H.; Looi, M.H.; Hamid, S.B.A. How important is the (001) plane of M1 for selective oxidation of propane to acrylic acid? *J. Catal.* **2008**, *258*, 35–43.
81. Schlogl, R. Selective oxidation: From a still immature technology to the roots of catalysis science. *Top. Catal.* **2016**, *59*, 1461–1476. [CrossRef]
82. Grasselli, R.K. Fundamental principles of selective heterogeneous oxidation catalysis. *Top. Catal.* **2002**, *21*, 79–88. [CrossRef]
83. Grasselli, R.K.; Buttrey, D.J.; Burrington, J.D.; Andersson, A.; Holmberg, J.; Ueda, W.; Kubo, J.; Lugmair, C.G.; Volpe, A.F., Jr. Active centers, catalytic behavior, symbiosis and redox properties of MoV(Nb,Ta)TeO ammoxidation catalysts. *Top. Catal.* **2006**, *38*, 7–16. [CrossRef]
84. Taylor, H.S. A theory of the catalytic surface. *Proc. R. Soc. London Ser. A* **1925**, *108*, 105–111. [CrossRef]

